Vol. 1, No. 1, pp. 18-23, December 2002

INTERNATIONAL JOURNAL OF SAFETY
www.kiis.or.kr

Development of a Three-Dimensional DNS Code for Study of Clean Agents

-Two-Dimensional Simulation of Diluted Nonpremixed Counterflow Flames-

Woe Chul Park* and A. Hamins[1]

**Department of Safety Engineering, Pukyong National University, Busan 608-739, Korea*
[1]Building and Fire Research Laboratory, National Institute of Standards and Technology Gaithersburg, MD 20899-8663, USA

(Received October 7, 2002; Accepted December 2, 2002)

Abstract : A mixture fraction formulation is used to numerically simulate the structure of diluted axisymmetric methane-air nonpremixed counterflow flames. The effects of global strain rate and gravity were investigated and results were compared. Fuel of a mixture of 20% methane and 80% nitrogen by volume and oxidizer of pure air at low and moderate global strain rates $a_g = 20$, 40, 80 s^{-1} in normal and zero gravity were computed. It is shown that the numerical method is capable of predicting the structure of counterflow flames in normal and microgravity environments at low and moderate global strain rates.

Key words : flame structure, counterflow flame, numerical simulation, normal and zero gravity

Nomenclature

a_g : global strain rate
c_P : constant pressure heat capacity
D : duct diameter (Fig. 1) or diffusion coefficient (Eq. 4)
g_o : gravitational acceleration constant, 9.81 m/s^2
G : dimensionless gravitational acceleration, g/g_o
H : size of y-direction computational domain
h : enthalpy
L : separation distance between ducts
M : molecular weight
Pr : Prandtl number, 0.7
Q : heat release rate per unit volume
R : gas constant
T : temperature
u : velocity
V : mean velocity at duct exit
V : velocity at duct exit
v : y-direction velocity
w : chemical production rate per volume
Y : mass fraction
Z : mixture fraction
δ_{ij} : Kronecker delta
λ : thermal conductivity
μ : viscosity
ν : stoichiometric coefficient
ρ : density
τ : shear stress

Subscripts

A : air
F : fuel
f : flame surface
O : oxygen
∞ : ambient

*Corresponding author: wcpark@pknu.ac.kr

1. Introduction

Although there have been many studies on the structure and extinction of moderately strained hydrocarbon diffusion flames, few studies have considered low strain rate flames. The exception to this is the recent work of Maruta *et al.* [1] and Hamins *et al.* [2] who investigated the extinction of low strain rate methane-air diffusion flames with N_2 added to the fuel stream under microgravity and normal gravity conditions, respectively. Both studies measured the critical conditions required to achieve extinction and numerically simulated

the counterflow flames using one-dimensional flame codes. For high strain rate conditions, buoyancy is overwhelmed by convection and the flames are thin and flat. For low strain rate flames in normal gravity, the high temperature reaction zone becomes thicker. As buoyancy forces become relatively more important, the flames become curved. In addition, while the microgravity flames are fairly flat, the one-dimensional steady state simulations fail to capture the dynamics of the flame during the transition from normal to microgravity.

The one-dimensional flame codes such as Rogg [3] and OPPDIF [4] are based on a similarity solution that neglects buoyancy. For physical insight, a numerical method is needed that is capable of simulating buoyancy dominated flows and is easily extended to multi-dimensional dynamics. The NIST Fire Dynamics Simulator (FDS) [5] was developed for predicting unsteady three-dimensional large-scale fire phenomena on a high-end Personal Computer. For grid sizes on the order of 5 cm to 20 cm, FDS employs a large eddy simulation (LES) method, in which the resolvable

large-scale eddies are computed directly and the sub-grid dissipative processes are modeled. FDS also employs the direct numerical simulations (DNS) for small-scale problems like the counterflow flames. In the present study, the grid is refined to sub-millimeter length scales and the code directly computes transport and dissipative process by using DNS.

Diffusion flames were simulated for normal and zero gravity conditions and different flow field strain rates. The main objective of the study was to investigate the effects of global strain rate and gravity. The effects of global strain rate and gravity on flame shape and temperature were investigated.

2. Methodology

Counterflow diffusion flames are formed between two opposed circular ducts separated by a distance L as shown in Fig. 1. Gas phase fuel, or a mixture of fuel and agent is supplied through the fuel duct, and air flows the oxidizer duct. Combustion between fuel and air is assumed to take place in quiescent nitrogen gas. In the present study, the oxidizer is composed of pure air and the fuel is composed of a mixture of 20% methane and 80% nitrogen by volume.

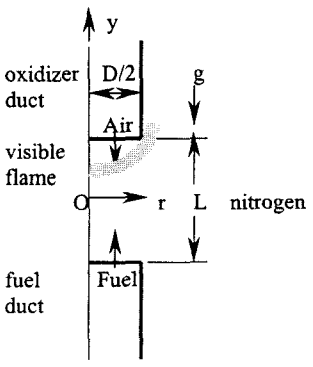

Fig. 1. Schematic drawing of the computational domain.

Assuming that the fluids are ideal gases, the governing equations are as follows [5]:

Conservation of mass:

$$\frac{\partial \rho}{\partial t} + \frac{\partial \rho u_i}{\partial x_i} = 0 \tag{1}$$

Conservation of linear momentum:

$$\frac{\partial \rho u_i}{\partial t} + \frac{\partial \rho u_i u_j}{\partial x_j} = -\frac{\partial p}{\partial x_i} + \rho g_i + \frac{\partial \tau_{ij}}{\partial x_j} \tag{2}$$

Conservation of energy:

$$\frac{\partial \rho h}{\partial t} + \frac{\partial \rho h u_i}{\partial x_i} - \frac{Dp}{Dt} = Q + \frac{\partial}{\partial x_i}\left(\lambda \frac{\partial T}{\partial x_i}\right) + \frac{\partial (u_i \tau_{ij})}{\partial x_i} \tag{3}$$

Conservation of species:

$$\frac{\partial \rho Y_i}{\partial t} + \frac{\partial \rho Y_i u_j}{\partial x_j} = \frac{\partial}{\partial x_j}\left(\rho D_i \frac{\partial Y_i}{\partial x_j}\right) + w_j \tag{4}$$

and

$$\tau_{ij} = \mu\left(\frac{\partial u_i}{\partial x_j} + \frac{\partial u_j}{\partial x_i} - \delta_{ij}\frac{2\partial U_k}{3\partial x_k}\right) \tag{5}$$

where, t represents time, ρ the density, u the velocity, τ the shear stress. D/D_t is the substantial derivative in Eq. 3, Q is the heat release rate per unit volume, λ is the thermal conductivity. Y is the mass fraction, D is the diffusion coefficient, w is the chemical production rate per volume, μ is the viscosity, δ_{ij} is the Kronecker delta. Pressure p is ρRT and enthalpy h is c_pT for ideal gases, where R is the gas constant, c_p is the constant pressure heat capacity, and T is temperature.

The boundary conditions on the velocity and temperature of the reactant stream are $V = V_F$ at the fuel duct exit, $V = V_A$ at the oxidizer duct exit, no slip condition at the duct wall, and $T = 300$ K in fuel and air streams in the ducts.

In the present study, radiation is not included and symmetry allows treating the flowfield as axisymmetric. The equations are solved for the velocity, temperature and species mass fractions from the discretized equations using an explicit method. The time step size is implicitly controlled such that the local Courant-Friedrich-Lewy (CFL) number (e.g., $v\Delta t/\Delta y$ in the y-

direction, where Δt is the time step and Δy is the y-direction grid size) is less than 0.5 avoiding instabililty and divergence problems. The solution procedures are described in detail in McGrattan *et al.* [5].

The mixture fraction model [6] is based on the assumption that the heat release rate is mixing controlled. In this manner, the model predicts the local heat release rate, the flame shape, the local temperature and other variables without the computational expense of detailed chemical kinetics. The fuel type influences the state relation, which is calculated for a one-step irreversible stoichiometric reaction of the following form:

$$\nu_O[O] + \nu_F[F] \rightarrow \Sigma \nu_P[P] \tag{6}$$

where O represents oxygen, F fuel, and P products. The mixture fraction Z is defined as:

$$Z = \frac{sY_F - (Y_O - Y_{O,\infty})}{sY_{F,d} + Y_{O,\infty}} \tag{7}$$

where $s = \nu_O M_O / \nu_F M_F$, the subscript O stands for oxygen, d duct, and ∞ ambient. M is the molecular weight, ν is the stoichiometric coefficient, Y is the mass fraction.

By definition, $Z = 1$ in a region of fuel only and $Z = 0$ where no fuel exists. On the flame surface, the reactants take on values $Y_O = 0$ and $Y_F = 0$, so Eq. 9 becomes:

$$Z_f = \frac{Y_{O,\infty}}{sY_{F,d} + Y_{O,\infty}} \tag{8}$$

where f stands for the flame surface. The relation between the oxygen mass fraction and Z is:

$$Y_O = Y_{O,\infty}(1 - Z/Z_f) \qquad Z < Z_f$$

$$Y_O = 0 \qquad Z > Z_f \tag{9}$$

The reaction of fuel and oxygen is released along an infinitely thin sheet where Z takes on its stoichiometric value as determined by Eq. 9. The heat release rate per unit area of flame surface is taken as directly proportional to the rate of consumption of oxygen. The calculated local temperature was not taken as being proportional to the mixture fraction, but instead was determined from consideration of the local heat release rate and the calculated local enthalpy including temperature dependent heat capacities. This approach assumes that finite rate kinetics does not significantly influence the calculated volumetric heat release.

3. Results and Discussion

The fuel is composed of 20% methane and 80% nitrogen by volume, and the oxidizer stream is composed of undiluted air taken as 21% oxygen and 79% nitrogen by volume. This corresponds to $Y_{F,d} = 0.125$, $Y_{O,\infty} = 0.23$, and $Z_f = 0.3151$.

For a given global strain rate (a_g), V_A and V_F are calculated by the definition of the global strain rate [7]:

$$a_g = \frac{2V_A}{L}\left[1 + \frac{V_F}{V_A}\left(\frac{\rho_F}{\rho_A}\right)^{0.5}\right] \tag{10}$$

In this study, three values of global strain rate $a_g = 20$, 40, 80 s^{-1} were computed. The velocity ratio V_A/V_F was set to 1 in all computations.

Based on an evaluation procedure, the computational domain was taken to be 40 mm in the r direction and 70 mm in the y direction for the duct diameter (D) and the separation distance (L) are 25 m, repectively (see Fig. 1), and the grid spacing was taken to be 0.5 mm in the both r and y directions. Computations with 80×140 grids typically required about 100 min on a PIII-650 Mhz PC with 256 MB RAM for 1.0 s of run time.

The global strain rate defined by Eq. 10 is an important parameter used in representing characteristics of the

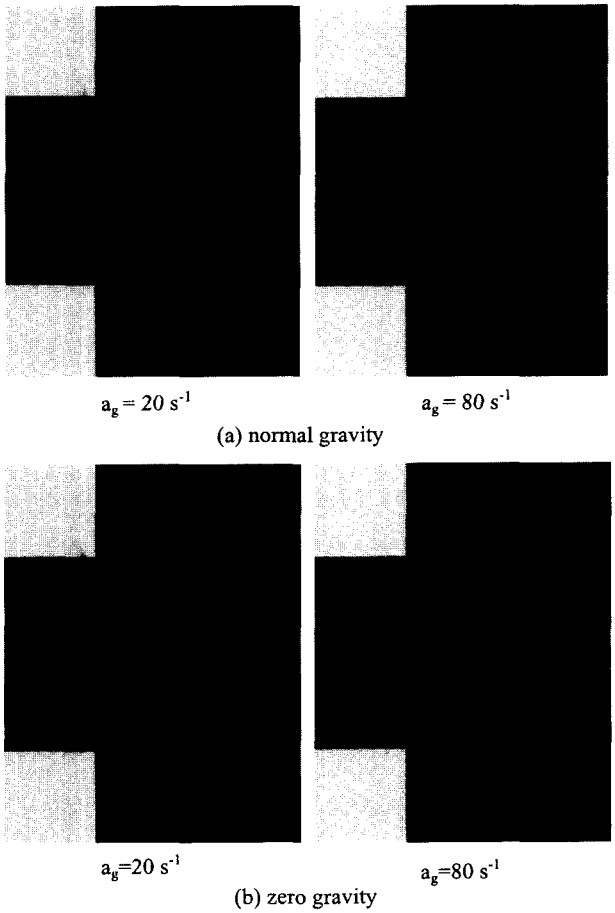

Fig. 2. Flames at $a_g = 20\ s^{-1}$ and 80 s^{-1}.

counterflow flames. Flame at low strain rates moves towards the upper oxidizer duct with low velocity and buoyancy at normal gravity. At the given fuel concentration and velocity ratio, the velocity at the duct exits is proportional to the global strain rate. To see if the present numerical method is capable of predicting the change in flame structure due to the global strain rate, temperature and velocity along the center line for low and moderate global strain rates, $a_g = 20\ s^{-1}$ ($V_A = V_F = 0.129$ m/s) and $80\ s^{-1}$ ($V_A = V_F = 0.515$ m/s) were compared at both normal gravity and zero gravity conditions.

Fig. 2 shows the flames at $a_g = 20\ s^{-1}$ and $80\ s^{-1}$ under normal and zero gravity conditions. The computational domain was 40×70 mm, but these figures show only 40×50 mm near the flame. Note that the one-dimensional codes does not provide any flame shape because they assume the flame one-dimensional. The flame shape clearly shows the difference due to different global strain rate. At $G = 1$ velocity at the duct exits is much smaller at the lower strain rate $a_g = 20\ s^{-1}$ than at $a_g = 80\ s^{-1}$. This makes the flame at the lower strain rate moves closer to the top oxidizer duct and the flame surrounds the duct surface. The smaller velocity also

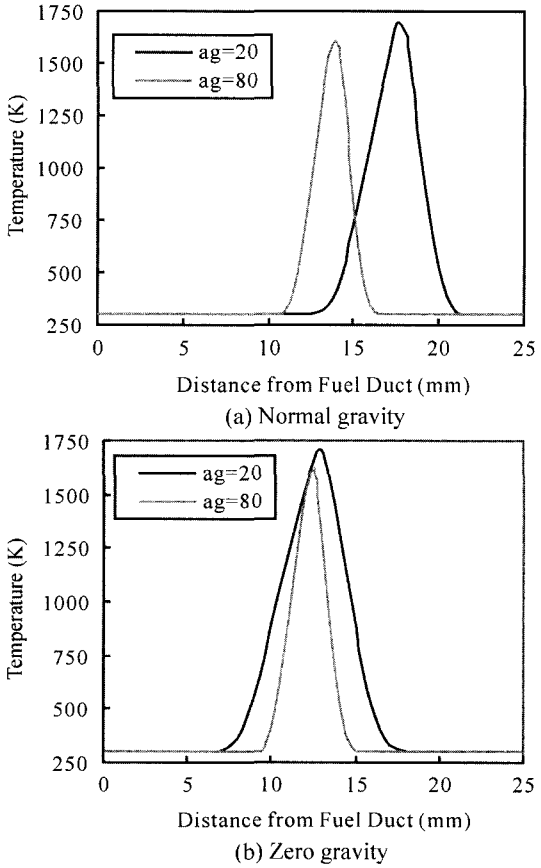

Fig. 3. Comparison of temperature and velocity for different values of a_g.

makes flame thicker. These results are also true under microgravity condition except that flame shift little at different strain rate due to no buoyancy at $G = 0$. At zero gravity, flame is sheet-like, particularly at the higher strain rate, $a_g = 80\ s^{-1}$.

Temperature is compared in Fig. 3 for the two strain rates. At normal gravity, as seen from the flames in Fig. 8, the flame moved towards the top oxidizer duct when $a_g = 20\ s^{-1}$, and the peak flame temperature decreased compared to $a_g = 80\ s^{-1}$: The peak temperature was 1696 K at 17.5 mm from the fuel duct exit at $a_g = 20\ s^{-1}$, whereas 1591 K at 14.0 mm at $a_g = 80\ s^{-1}$, but. This difference is due to low axial velocity and high buoyancy at the lower global strain rate. The stagnation point was at 16.5 mm from the fuel duct exit at $a_g = 20\ s^{-1}$, and 13.0 mm at $a_g = 80\ s^{-1}$. It can be seen when $G = 0$ that the temperature difference is almost same as the case at $G = 1$, but the effects of strain rate at zero gravity are much weaker than at normal gravity. The location of flame is not shifted so much as at normal gravity. There was a small difference at the stagnation point. It is also noted in Fig. 3 that at both the normal and zero gravity conditions, the smaller strain rate yields a thicker flame. The lower axial velocity results in increase in flame thickness.

Under low momentum conditions, buoyancy is relatively more important and significantly effects flame structure Buoyancy is directly related to the two terms on the right hand side of Eq. 2, $\partial p/\partial x_i$ and ρg_i. Accurate prediction of these terms is very important since all fires are strongly driven by buoyancy in normal gravity.

In Fig. 2, the normal gravity flame located closer to the oxidizer duct due to the presence of buoyancy, whereas the zero gravity flame was a horizontal sheet symmetrical about the r-axis for both global strain rates. The flame at zero gravity was thicker than at normal gravity, and the position of the flame was shifted downward at zero gravity.

The effects of gravity, that are characterized as changes in flame thickness, peak temperature, and the location of stagnation point can be confirmed more clearly from the profiles of temperature and axial velocity along the centerline as shown in Fig. 3. The peak temperature and the stagnation point are shifted downwards towards the middle of the domain for zero gravity. The peak temperature increases little at zero gravity. The flame at zero gravity is thicker than normal gravity, particularly at a low global strain rate.

Fig. 4 shows flames of $a_g = 40\ s^{-1}$ at normal and zero gravity at the velocity ratio $V_A/V_F = 1$. Compared to the flames in Fig. 2, the curvature of the flame at normal

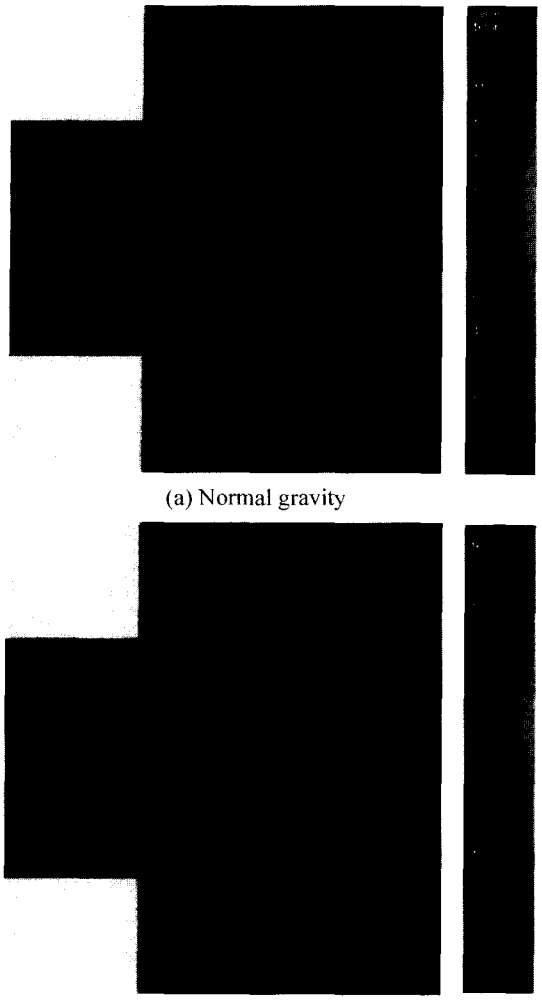

(a) Normal gravity

(b) Zero gravity

Fig. 4. Flames computed at $a_g = 40\ s^{-1}$.

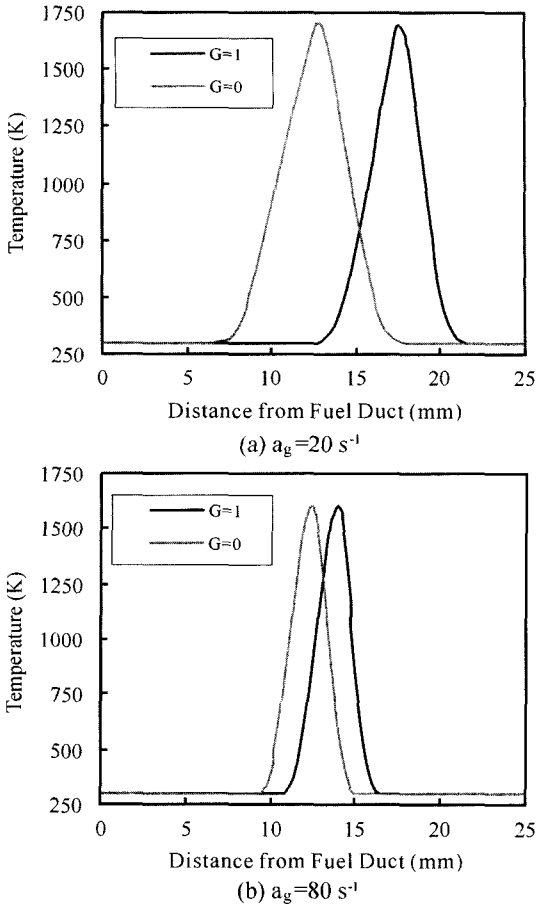

Fig. 5. Comparison of temperature and velocity at normal and zero gravity.

gravity and its thickness at zero gravity are between those of $a_g = 20\ s^{-1}$ and $a_g = 80\ s^{-1}$. This comparison of flame shape shows that the diffusion flame cannot be assumed to be one-dimensional at normal gravity, and that radiative heat transfer in the radial direction may increase as the global strain rate decreases due to increase in the flame thickness.

In Fig. 5, the peak temperature is shifted towards the middle of the domain for $G = 0$. The peak temperature increases little at zero gravity. The flame at zero gravity is thicker than normal gravity, particularly at the lower global strain rate. Change in the peak flame temperature is not significant at the both strain rates. The effects of buoyancy at $a_g = 80\ s^{-1}$ are much smaller than at $a_g = 80\ s^{-1}$ It can be seen that the effects of gravity are more important at low global strain rates.

Although the two-dimensional simulation was evaluated at limited cases, the method is shown to be capable of predicting the effects of the global strain rate and buoyancy on flame structure. The popular one-dimensional flame code OPPDIF [4] does not provide valuable information on the flame shape and the effects of gravity. Because of this, the two-dimensional simulation may provide physical insight and be a useful tool for experiments on the counterflow flames.

4. Conclusions

A two-dimensional numerical simulation with a mixture fraction combustion model was applied to diluted counterflow methane-air diffusion flames. The temperature and axial velocity profiles for $G = 0$ showed reasonable agreement with the results of a one-dimensional flame code. The method is then exercised to evaluate the effects of varying levels of gravity and local strain rate. It is shown that the numerical method is capable of predicting the structure of counterflow flames in normal and microgravity environments at low and moder-

ate global strain rates. The computed structure of the zero gravity counterflow flames show large differences with those under normal gravity conditions.

Acknowledgement

This work was supported by Pukyong National University Research Abroad Fund in 2001.

References

[1] K. Maruta,, M. Yoshida, G H. Uo, Y. Ju and T. Niioka, "Extinction of Low-Streched Diffusion Flame in Microgravity", Combustion and Flames, Vol. 112, pp. 181-187, 1998.

[2] A. Hamins, M. Bundy, I. K. Puri., K.B. McGrattan and W.C. Park, "Suppression of Low Strain Rate Nonpremixed Flames by an Agent", Proc. 6th Intl Microgravity Combustion Workshop, pp. 101-103, 2001.

[3] B. Rogg, "A Computer Program for the Simulation of One-Dimensional Chemically Reacting Flows", Technical Report CUED/A-THERMO/TR39, Univ. of Cambridge, Dept. of Eng., 1991.

[4 A., Lutz, R.J. Kee, J. Grcar and F.M. Rupley, "A Fortran Program Computing Opposed Flow Diffusion Flames", SAND96-8243, Sandia National Laboratories, Livermore, CA, 1997.

[5] K.B. McGrattan, H.R. Baum, R.G. Rehm, A. Hamins, G.P. Forney, J.E. Floyd, S. Hostikka, "Fire Dynamics Simulator Technical Reference Guide", v.2, National Institute of Standards and Technology, Gaithersburg, MD, 2001 (see http://fire.nist.gov/fds).

[6] J.E. Floyd, K.B. McGrattan and H.R. Baum, "A Mixture Fraction Combustion Model for Fire Simulation Using CFD", Proc. Intl Conf. on Engineered Fire Protection Design, pp. 279-290, 2001.

[7] K. Seshadri and F.A. Williams, "Laminar Flow Be-tween Parallel Plates with Injection of a Reactant at High Reynolds Number", Intl J. Heat Mass Transfer, Vol. 21, pp. 251-253, 1978.